Metrol. Meas. Syst., Vol. 27 (2020) No. 4, pp. 641–657
DOI: 10.24425/mms.2020.134844

METROLOGY AND MEASUREMENT SYSTEMS
Index 330930, ISSN 0860-8229
www.metrology.wat.edu.pl

BEHAVIOR OF SINGLE-POINT HARMONIC PRODUCER INDICATORS IN ELECTRIFIED AC RAILWAYS

Andrea Mariscotti

University of Genova, DITEN, Via Opera Pia 11A, 16145 Genova, Italy (✉ *andrea.mariscotti@unige.it*, +39 0103 532 169)

Abstract

Electrified railways are an example of AC single phase distribution networks. A non-negligible amount of active and nonactive power may be related to harmonics, especially for distorted highly-loaded systems. The paper considers the relevance of the harmonic power terms in order to identify distortion sources in a single-point perspective, in line with the approach of EN 50463 for the quantification of the power and energy consumption. Some single-point Harmonic Producer Indicators (HPI) based on harmonic active power direction and nonactive distortion power terms are reviewed and evaluated using pantograph voltage and current measured during several hours of runs in two European AC railways (operated at 16.7 and 50 Hz). The HPI based on active power shows to be consistent and provides detailed information of rolling stock characteristic components under variable operating conditions; those based on nonactive distortion power are global indexes and hardly can operate with complex harmonic patterns in variable operating conditions.

Keywords: distortion power, electric transportation systems, harmonic source, Power Quality, power system harmonics, railways.

1. Introduction

Electrified railways are an example of AC single-phase distribution networks characterized by a significant amount of distortion (when compared to most medium voltage distribution networks) with moving loads (the trains), featuring very dynamic operating profiles (acceleration, cruising, coasting, and braking). A single train is also a combination of different on-board loads, from the traction drive to the auxiliaries for technical and hotel services (apparatus ventilation, compressed air, air conditioning, lighting, *etc*.).

Harmonic propagation in electric railways is responsible for phenomena of induced voltage and interference to signaling, more than conducted disturbance along the feeding network that is quite robust in this sense [1]. A new perspective is considering their effect in terms of power flow, its measurement and billing. Besides the fundamental (16.7 Hz, 50 Hz, 60 Hz), also harmonics

may be relevant for the active and reactive power exchange [2–5]. With the introduction of energy metering on-board [6, 7], a definition is necessary of active and reactive power concepts that is valid for the fundamental and harmonics, which should be taken into account to satisfy the requirements of accuracy and uncertainty [7].

In general, modern trains complying with the EN 50388 power factor limit [8] have current spectrum components [9, 10] smaller by an order of magnitude than those used to test immunity of onboard energy meters (EN 50463-2 [7]). In addition, a minimum power factor of 0.85 appears in Table 3 of the EN 50463-2. Besides this power factor limitation, railway standards contain no other prescriptions or characterizations for harmonic distortion of rolling stock or traction supply: the new draft of the EN 50388-1 [11] implicitly explains this lack with the complexity of the system and the need for a specific compatibility study. It is possible thus to identify two factors relevant to assessment of the energy consumption, energy efficiency and fair billing:

- accurate measurement and evaluation of harmonic power components to be included in the determination of the so-called *Energy Measurement Function* (EMF), discussed in [2–5], assessing the relevance of harmonic power components and the impact on EMF uncertainty;
- identification of harmonic power sources with suitable indicators, able to clearly represent the amount of distortion and to determine if some train is an active source pulling power at some harmonics or just a passive load for the line voltage distortion caused by other trains or substations [12], including possible forms of cost sharing and billing [13]; other methods based on interpretation of spectra and waveforms are shown in [14]. An interesting discussion of the effect of distortion on the operation of energy meters can be found in [15–18].

In view of relevance of the harmonic power components for the calculation of the consumed and regenerated power and energy [2–5], this work aims at determining suitable methods for the identification of power sources in electrified railways in a single-point metering perspective. The advantages of single-point detection may be synthesized as follows: unlike multi-point methods it does not need distributed and synchronized measurements, it is compatible with a scenario of moving sources of different types and thus a continuously reconfiguring network, and it can be more easily implemented in existing hardware that measures energy consumption based on the local pantograph electrical quantities.

2. Power model and power related quantities

Definitions and discussions of terms can be found in several works [19–27] and in the IEEE Std. 1459 [28], and they will not be extensively repeated here; what is relevant is the definition and behaviour of harmonic nonactive power terms for distorted waveforms. These terms, starting from the definition of the instantaneous power in the time domain, are well described in [22, 23]. The expressions for single-phase systems shown in [22], sec. III.A, well adapted to AC railways and will be considered further, so as to offer a comprehensive representation of all non-fundamental terms and their relationships in non-sinusoidal situations. Starting from the instantaneous voltage and current waveforms (neglecting DC components):

$$\begin{aligned} v(t) &= \sqrt{2}V_1 \sin(\omega t - \alpha_1) + \sqrt{2}\sum_{h\neq 1} V_h \sin(h\omega t - \alpha_h), \\ i(t) &= \sqrt{2}I_1 \sin(\omega t - \beta_1) + \sqrt{2}\sum_{h\neq 1} I_h \sin(h\omega t - \beta_h). \end{aligned} \tag{1}$$

Metrol. Meas. Syst., Vol. 27 (2020), No. 4, pp. 641–657
DOI: 10.24425/mms.2020.134844

The resulting terms when voltage and current waveforms are multiplied to derive the instantaneous power $p(t) = v(t)\ i(t)$ are:

$$p_a = \sum_h V_h\, I_h \cos\vartheta_h\, [1 - \cos(2h\omega t - 2\alpha_h)], \tag{2}$$

$$\begin{aligned} p_q &= -\sum_h V_h I_h \cos\vartheta_h [1 - \cos(2h\omega t - 2\alpha_h)] + 2\sum_m \sum_{m\neq n} V_m I_n \sin(m\omega t - \alpha_m)\sin(n\omega t - \beta_n) = \\ &= -\sum_h V_h I_h \cos\vartheta_h [1 - \cos(2h\omega t - 2\alpha_h)] + V_1 \sum_h I_h \sin(\omega t - \alpha_1)\sin(h\omega t - \beta_h) + \\ &+ I_1 \sum_h V_h \sin(h\omega t - \alpha_h)\sin(\omega t - \beta_1) + 2\sum_{m>1} \sum_{\substack{n>1 \\ m\neq n}} V_m I_n \sin(m\omega t - \alpha_m)\sin(n\omega t - \beta_n). \end{aligned} \tag{3}$$

The p_q term has its parts that can be recognized as deriving from multiplication of two components of the same harmonic order h, of two components of different harmonic orders m and n, and one component of harmonic order h with the fundamental (exchanging the roles of voltage and current). For AC railways DC components initially appearing in (1) are excluded for simplicity, as they in principle should not appear: in reality, DC may arise from transients (in the electrical system) and from uncompensated offsets (in the measurement system), besides introducing the complication of DC-coupled transducers to carry out such measurement.

In an AC railway system the sources of distortion are: the substation (feeding the system with the distortion occurring at the high voltage level upstream), the *Train Under Test* (TUT) (which sees the *Point of Common Coupling*, PCC, positioned at the pantograph, where a mix of internal and external harmonic terms takes place), and the remaining trains in the same supply section (whose on-board sources may be synchronized with the fundamental and whose harmonic emissions may superpose with some phase rotation, depending on frequency and distance from TUT [29]). Phase angle rotation is in general crucial for the interpretation of data from Phasor Measuring Units and their optimal placement, as pointed out in [30].

Active power terms at the fundamental P_1 and harmonics P_h sum up and give the total active power P_t with a clear physical meaning. Nonactive power terms, conversely, are only conventionally summed, agreeing on a quadrature sum to indicate, as is known, the intensity of the overall flowing current with no active power associated to it. Although active power terms are in general the most relevant, reactive power terms have an indirect active effect [31-33], causing increased losses in the traction supply line, but mostly in cables and static machines on-board and at substations (with secondary effects of ageing and reduced service life [34]).

The overlapping of the harmonic patterns of the various sources cannot exclude partial cancellation of some terms, resulting in a lower nonactive power. Practically speaking, distortion components from different, but similar, sources (*e.g.* locomotives of the same type/model) will overlap and due to the arbitrary phase rotation along the traction line observed in [29], partial cancellation is possible, although unlikely.

3. Harmonic Producer Indicators (HPIs)

The attention is focused on single-point detection methods, rather than multi-point methods, for the following reasons:

– multi-point methods require distributed and synchronized measurements;

– trains are a moving source, and multi-point methods would need precise and updated info of their location to update the network model, in addition to measuring electrical quantities at the interfaces of all involved rolling stock items;
– a supply section of a traction line sees different types of rolling stock at the same time from different manufacturers, thus with different implementations of the same EN 50463-2 protocol in a single-point perspective without information necessary to implement multi-point methods;
– a single-point method, if effective, is much simpler and preferable, also from the standpoint of promoting its adoption and implementation.

Another peculiar characteristic of electrified railway systems is that they are an intermediate case with respect to the two extreme situations of a non-sinusoidal supply voltage feeding a linear load and a sinusoidal supply voltage feeding a non-linear distorting load, that are usually implicitly considered for HPIs in industrial and public networks. Additionally, non-sinusoidal loads pulling distorted current interact with the network impedance at the pantograph that varies with the train position and is far from the condition of a stiff source: distortion amplification and resonance conditions are well-known problems of modern ac railways [9, 10, 35].

The following methods and indicators have appeared in the literature over the last thirty years: they use various active and nonactive power formulations and terms; their behaviour will be then evaluated specifically for AC railways.

3.1. Active Power Indicators

The sign of the harmonic active power components (the so called "power direction method") was considered a good indicator (a negative sign indicates that a load is a source of harmonics carrying active power) until Xu [21] showed some inconsistency. The inconsistency is confirmed by the tests on simulated data in [25], sec. III and Fig. 7, where not only the wrong indication of the sign of the active power is remarked, but also the very small amplitude compared to nonactive power terms that can cause problems of accuracy in real scenarios. Although not a fully reliable indicator, it can still be used, possibly in combination with other indicators, since it is quite informative and can distinguish single harmonic components. This method is indicated as *Active Power Indicator* (API).

3.2. Nonactive Power Indicators

From (3), the consideration of the mutual products between harmonic components of voltage and current makes it possible to separate the set of nonactive power components with various criteria: the fundamental and harmonics, and of the latter, those in common to voltage and current and those that appear only in one of the two (following Sharon's definition [36]). The same authors [22, 23] proposed two single-point methods based on different uses of the following quantities: Fryze's reactive power Q_F, Sharon's quadrature reactive power Q_S. The term Q_1 will be used in the following to indicate the fundamental reactive power.

$$Q_F = \sqrt{S^2 - P^2}, \quad Q_S = V_{rms}\sqrt{\sum_{h\in C} I_h^2 \sin^2(\theta_h)}, \quad Q_X = V_{rms}\sqrt{I_1^2 \sin^2\theta_1 + \sum_h I_h^2 \sin^2\theta_h}, \quad (4)$$

where θ_1 and θ_h are the differences of phase between voltage and current between the fundamental and harmonics, with $\theta_h = \beta_h - \alpha_h$, and with "$h \in C$" we have indicated the set of harmonics common to both voltage and current. The notation in the original Sharon's paper [36] is ambiguous

for h to include the fundamental or not. Similarly in [22] the authors say "harmonics common to voltage and current", that would exclude the fundamental ($h = 1$). The interpretation and discussion in both references then clarifies that the fundamental is included.

The methods will be identified as *Reactive Power Interval Indicators* (RPII), using Q_X (thus RPII-X) and using Q_S (thus RPII-S); the methods can be detailed as follows:

RPII-X) the comparison of Q_1 (minimum of nonactive power), Q_X and Q_F (maximum of nonactive power) leads to creation of the following rules [23]:

- rule 1: with network distortion and non-linear loads the three quantities are different;
- rule 2: when network distortion is predominant and the distorted current pulled by the nonlinear load is smaller, then Q_1 and Q_F are closer, and Q_X is closer to Q_1 than to Q_F;
- rule 3: symmetrically, when network distortion is smaller and the nonlinear load absorbs a significant distorted current, then Q_X is closer to Q_F than to Q_1.

RPII-S) the comparison of Q_1 (minimum of nonactive power), Q_S and Q_F (maximum of nonactive power) leads to creation of the same rules used for RPII-X above [22].

A third method was also proposed in [27], named *Distortion Power Indicator* (DPI) and based on the calculation of the Distortion Power D, taken from the total apparent power S by subtracting in a quadratic way the active and reactive power at the fundamental and harmonic components (P_1, Q_1, P_h, Q_h, h spanning all harmonics); the term D corresponds to the power terms originating from the mixed products of components at different frequency.

$$D = \sqrt{S^2 - P^2 - \sum_h P_h^2 - Q_1^2 - \sum_h Q_h^2}\,. \tag{5}$$

The authors underline that the proposed indicator does not fail to detect distortion caused by non-linear loads and there are no cases in which a load is wrongly tagged as a distorting load. They also demonstrate that in the case of a linear load there may be errors in the determination of D, indicating instead a small, but non-null, value. Thus, they suggest disregarding any contribution below a given convenient threshold to avoid the observed inaccuracy for small values. No explicit rules are given in [27] to evaluate the behavior of this indicator and its range of variation except that a non-null (and positive) value of D indicates the presence of a distorting load.

DPI) the definition of D leads to generating the following rule:

- rule 1: in the presence of network distortion D is significantly greater than 0.

3.3. General considerations on Active and Nonactive Power Indicators

The first problem of the RPI and DPI indicators is that they are global indicators, quantifying the overall distortion due to uncommon harmonics, unable thus to establish if a load is the source of a specific harmonic, as harmonic terms in all real situations are mixed: some are caused by the network (possibly by nearby loads) and some can be traced back to the specific load under examination (the TUT).

In general, an observation can be extrapolated to all methods while speaking of uncommon harmonics i.e. in real cases there are not really harmonic terms that might appear in the voltage and not in the current, or vice versa, as the interaction with the network and load impedance (extending for convenience the concept of impedance also to non-linear loads) will always produce a voltage harmonic starting from a pulled current harmonic, and vice versa. Of course, this process results in a wide range of amplitudes that in some cases may be masked by network and instrumentation noise, so as to say that a specific harmonic is present only in one of the two vectors and it is thus "uncommon". Based on this consideration, there is an inherent difficulty in identifying the set C

in a real case. For this reason, the index RPII-S based on Q_S is approximated to RPII-X and will not be explicitly calculated.

It is interesting also to test these three nonactive power indicators in the presence of a reversed power flow, as in the case of regenerative braking, that is quite common in railways, with fast dynamics between consumer and producer conditions.

3.4. Indicators requiring additional information on the network and the load

There are other methods that, despite being single-point methods, require additional information regarding the impedance of network and load.

- The methods described in [37] for the cited references "Xu-Liu, 1999" and "Chaoying, 2004" require the knowledge of the network and load impedance and are not thus applicable to the present case, where the variability of the network impedance present at the pantograph during the train journey is the critical aspect (see below);
- Other methods described in [37] as THD (from the referenced paper "Costa, 2009") and harmonic vector method ("Pfaifar, 2008") suffer from unpractical harmonic modeling and inability to determine the location of harmonic sources at individual harmonic frequencies;
- The RLC method proposed in [37] models the load by three parallel branches forming a RLC circuit, but does not clarify if and how the network (or utility) impedance is modelled, although it appears in the proposed equations.

In general, the network impedance of DC and AC railways present at the pantograph is quite variable, alternating resonances and anti-resonances in a well-known pattern [9, 38], established by the behaviour of the line as a multiconductor transmission line, with additional influence from lumped loads (such as substation filters, other trains, auxiliary transformers, *etc.*) [39].

The estimation of the network impedance could be ideally achieved just as outlined in [40]. An ideal step change of the network voltage is exploited there to evaluate the network impedance, by measuring the re change of absorbed current in the load (assuming that load conditions do not vary during the network transient). Since the network voltage is not under control and switching a lumped load in and out is not trivial (with several issues related to the cost, electrical safety, rating and certification), an effective implementation needs to be identified [41]. Railway systems are rich in power supply transients that could be exploited to this aim, such as pantograph arcs [42–44] and switching of auxiliary loads and onboard devices [41]. Impedance identification has been attempted for DC systems in a well-known configuration (onboard filter charging) for which the network equivalent circuit can be separated, but it is not readily extendable to AC railways, since the exploited transient is peculiar to a specific operation on DC networks.

3.5. Selected Harmonic Producer Indicators

To summarize, API method and RPII-S and RPII-X methods are well understood, can be easily implemented and do not rely on information regarding system impedance. As suggested in [22], API may be used in conjunction with RPII for a more reliable indication. In addition, the DPI method exploits the cross products between components at different frequencies, pointing directly at the superposition of current distortion pertaining to loads and voltage distortion characterizing the network. The above indicators are tested against various configurations and train operating conditions using the Swiss and Italian networks as examples [9, 10] the former is a 15 kV 16.7 Hz system featuring mixed traffic and a complex superposition of contributions, whereas the latter is a 2×25 kV 50 Hz high-speed line with a small number of well-separated trains.

Metrol. Meas. Syst., Vol. 27 (2020), No. 4, pp. 641–657
DOI: 10.24425/mms.2020.134844

4. Evaluation of HPIs in AC railways

The measured data consist of pantograph voltage and current in well-defined operating conditions with known type of the locomotive, so that the operating principles and characteristics are sufficiently known, in order to support the recognition of harmonic patterns. Trains are sources of different harmonic patterns caused by various non-linear loads on-board, with variable intensity depending on the operating conditions. Trains of the same type can be considered as having the same harmonic pattern if in the same or similar operating conditions [14]; otherwise, differences may be observed, such as between traction and braking (which in AC rolling stock occurs with the use of the same four-quadrant converter) or the contribution of auxiliaries especially during coasting and at a standstill. As anticipated, partial cancellation of some components is possible in the presence of more than one instance of the same model of rolling stock. This is not unusual if we consider that fact that regional and commuter trains of the same operator are probably pulled by the same type of the locomotive, while the fleet of high-speed trains is typically composed of many different models.

Pantograph voltage and current waveforms are available in [45], arranged in a dataset, where tags indicate train operating conditions (traction, braking and standstill) and speed. Each sample has the time duration of five cycles, sufficient for the calculation of power terms and HPIs: to this aim the DFT window T is set to 300 ms for five cycles of the 16.7 Hz fundamental and 100 ms for the 50 Hz system. Characteristic harmonics are well separated by a frequency resolution that is one fifth of the fundamental frequency; they are then extracted to feed the HPI algorithms. It is observed that the selected time windows are in agreement with the fastest time step adopted for electromechanical simulation [47, 48], indicating that the train kinematics can be satisfactorily tracked and its mechanical quantities may be assumed constant over the T interval. Original data were sampled at 50 kS/s, ensuring sufficient oversampling even at the highest harmonics covered by this analysis, set to 5 kHz for convenience and in agreement with previous works [2–5]. Each window T is transformed using a Hann window to control spectral leakage.

The data were acquired during a long measurement campaign in 2007 and 2008 synthetically described in [9] where voltage and current sensors and the data acquisition system are described, together with their basic metrological characteristics. The data acquisition system (a 16-bit digitizer) has a negligible influence on the overall uncertainty budget. The voltage and current sensors consisted of a capacitive divider and a Rogowski coil, respectively. Amplitude accuracy was unavoidably affected by installation variability, besides gain flatness (estimated as less than a worst-case 1% overall with coverage factor $k = 1$). Regarding the phase response, it should be stressed that the sensing principle for both sensors is intrinsically linear i.e. non-linearity may emerge at the extreme of the respective band, around 5 Hz and at 10 kHz, from which arises the limitation of the analysis to 16.7 Hz – 5 kHz. The Rogowski integrator may cause some linearity issues at low frequency for which it was tested with a square wave i.e. the deviation was 1.1% excluding the portions at and after the rise and fall edges, where deviations are due to band limitations. No additional filters were used which could have brought in a non-linear phase response, especially around the corner frequency.

Phase angle uncertainty has a direct influence on the breakdown in active and reactive power terms, observing that amplitude uncertainty would have a moderate influence on the overall value of apparent power. The angle θ (difference of voltage and current angles) can be affected with a variable error caused by different responses of the voltage and current sensors built in different technologies, but using linear physical principles and tested with the square wave. Unfortunately, no direct calibration of the phase response was carried out.

The calculated HPIs are shown in Figs. 1–6 for the two railway systems, focusing on API (active power) and RPII and DPI (nonactive power). RPII and DPI indexes are also expressed as fractions of the maximum nonactive power Q_F for ease of interpretation.

Since the API index is built on the calculation of active power for each harmonic component (indicated by the harmonic order in ordinate in Figs. 1 and 2, a suitable representation is based on

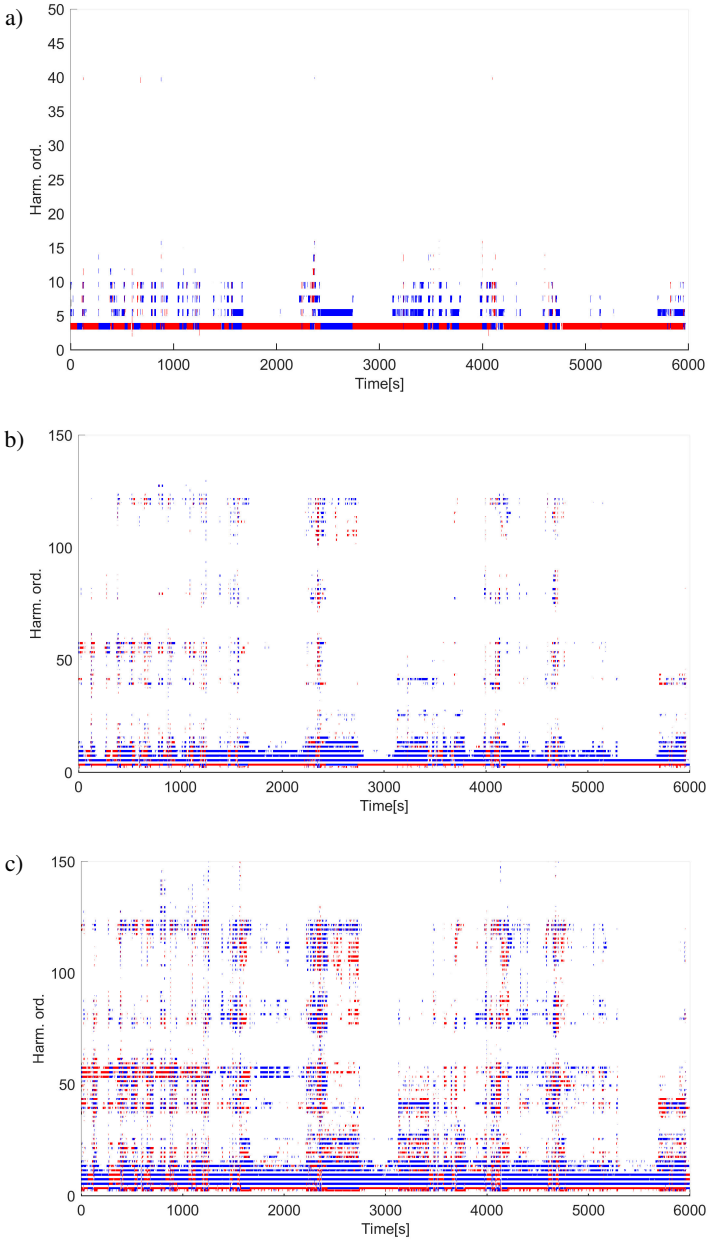

Fig. 1. Distribution of the API index vs. harmonic order and time for (a) 99.5%, (b) 98% and (c) 95% percentiles reporting positive (red, into the rolling stock) and negative (blue, out of the rolling stock) P_h values (Switzerland).

Metrol. Meas. Syst., Vol. 27 (2020), No. 4, pp. 641–657
DOI: 10.24425/mms.2020.134844

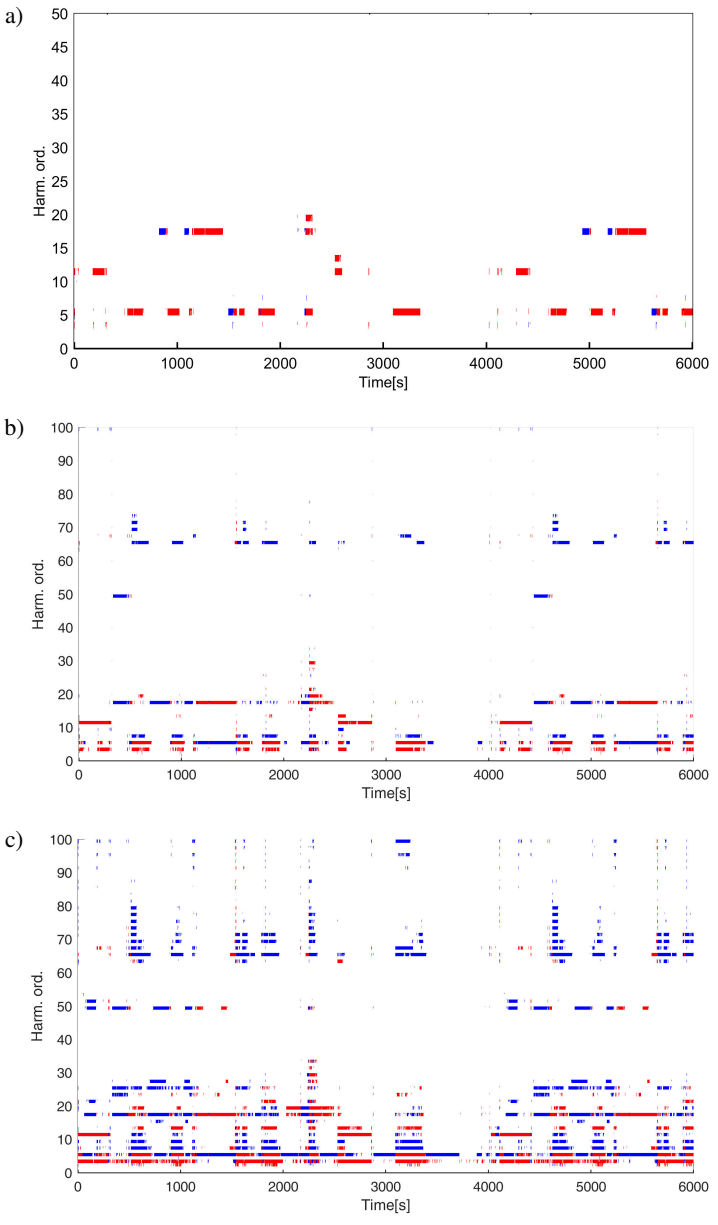

Fig. 2. Distribution of the API index vs. harmonic order and time for (a) 99.5%, (b) 98% and (c) 95% percentiles reporting positive (red, into the rolling stock) and negative (blue, out of the rolling stock) P_h values (Italy).

displaying how many components have active power above a significance threshold together with their sign i.e. values are dispersed, so percentiles are used, retaining the most relevant components in terms of P_h intensity (regardless of its sign). The distribution of the relevant components is shown in Figs. 1 and 2, with 95%, 98% and 99.5% percentiles selected to enhance the graphical representation with clearly visible characteristics; the sign of the API index is also displayed

indicating in red positive values (into the rolling stock) and in blue negative values (out of the rolling stock).

First of all, it is worth noting that relevant harmonics are limited to maximum a 5% of the spectrum, with the 95% of the spectrum components adding second-order details to harmonic patterns already recognizable using those of the higher percentiles. The API index proves extremely useful while spotting the harmonic patterns composition and to distinguish the power flow between the network and the rolling stock. In [14] it is demonstrated that scatter plots and x–y diagrams of harmonic power have more information than those elaborated on voltage and current components (such as Lissajous diagrams and instantaneous impedance). Low-order harmonics are the largest ones and they are in general caused by network distortion with one exception i.e. the 50 Hz component in the Swiss network is not only the 3-rd harmonic of the network fundamental, but is also a by-product of onboard and substation transformers' non-ideal characteristics. In addition, it is used to supply auxiliaries onboard, so that a distinct power flow can be observed at this frequency (see *e.g.* in Fig. 1, the opposite behaviour of the 3-rd and the other odd low-order harmonics, almost always with opposite direction, alternating red and blue). Instead, in the 50 Hz system there is a prevalent 5-th harmonic that alternates with the 1-th and 17-th with a unidirectional incoming active power flow.

In the 99% percentile the characteristic harmonic patterns of onboard traction drives are already visible, adding to the low-order harmonics already appearing in the 99.5% percentile i.e. they are located at 800 and 2000 Hz for the Swiss case, and about 900 and 2500 Hz for the Italian case, with an additional set of components around 3250 Hz. These different switching frequencies are characteristic of both the TUT onboard traction converters and other trains causing distortion within the same supply section.

Taking for example Fig. 1c and the components around 800 Hz (odd components around the 48-th harmonic of the 16.7 Hz fundamental), they distinguish from those at 2000 Hz (known to be caused by a different type of train serving the same line) i.e. the former are prevalently red and more persistent, the latter are blue and sparser; in addition, the amplitude is larger for the endogenous power terms. Considering time evolution, it is possible to see there are bursts of higher values of harmonic power components that are common to the endogenous and exogenous sources, this because there are time intervals in which the locomotive input impedance is particularly low and this amplifies the intensity of current components and, as a consequence, the amplitude of related harmonic power components terms of either origin.

Several vertical bursts with a precise time location can be observed, during which there is a general increase of P_h at the characteristic and low-order harmonics. These events are not pure transients such as electric arcs [41–44], because the spectrum is not polluted by non-characteristic harmonics with a flat quasi-white behaviour; rather they are transient conditions of train operation. It is worth noting in Fig. 1 that during such bursts P_3 reverses its sign, indicating thus a braking phase. This is confirmed by inspecting the i_p waveform and the speed profile. Similar bursts can be seen in Fig. 2, but they are fewer and with longer duration, this is justified when one considers that the 50 Hz system is a high-speed line with a more regular speed profile, with less but more intense decelerations that cause a higher energy exchange.

Figs. 3–6 show the nonactive power indexes RPII-X (Q_X) and DPI (D). For display purposes the HPIs are shown normalized by means of u and v against the two reference quantities Q_1 and Q_F:

$$u_F = Q_F/Q_1\,, \qquad u_X = Q_X/Q_1\,, \qquad u_D = D/Q_1\,, \tag{6a}$$

$$v_1 = Q_1/Q_F\,, \qquad v_X = Q_X/Q_F\,, \qquad v_D = D/Q_F\,. \tag{6b}$$

Metrol. Meas. Syst., Vol. 27 (2020), No. 4, pp. 641–657
DOI: 10.24425/mms.2020.134844

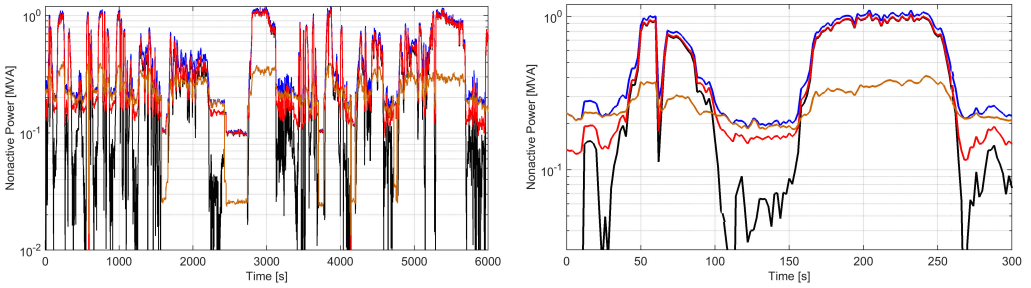

Fig. 3. Nonactive HPIs: Q_1 (black), Q_F (blue), Q_X (red), D (light brown) (Switzerland).

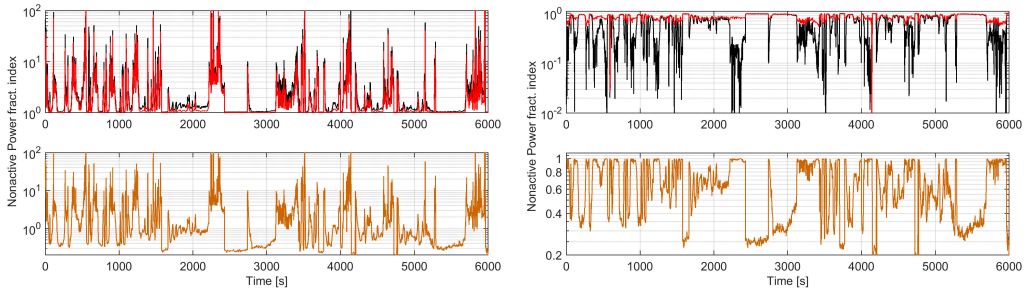

Fig. 4. Nonactive HPIs: Q_1 (black), Q_F (blue), Q_X (red), D (light brown) (Italy).

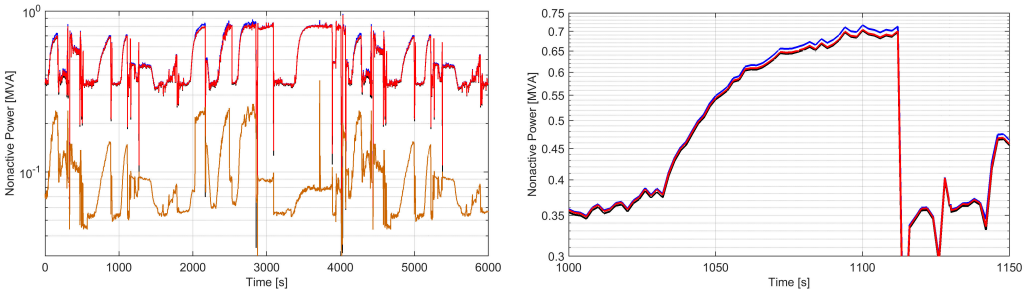

Fig. 5. Nonactive HPIs over a long run normalized to Q_1 (left, u_F (black), u_X (red), u_D (light brown)) and to Q_F (right, v_1 (black), v_X (red), v_D (light brown)) (Switzerland).

We observe that during significant power absorption the fundamental reactive power Q_1 prevails and Q_X is observed closer to Q_1 (see *e.g.* Fig. 3, right, between approximately 50 and 100 s, and 160 and 250 s); the second term composing Q_X is in fact small. This term can approximately correspond to Q_S on the assumption that line voltage distortion is small and thus V_1 and V_{rms} are quite similar. In this case, RPII-X is correct, since the observed reactive power Q_1 is in fact pulled by the train. As Q_S contains a fraction of the distortion terms in D, its value is always smaller. During low power absorption, such as coasting and standstill, the two almost coincide. Observing Fig. 3 (right), one can also notice that for Switzerland the D curve (light brown) almost touches Q_F (blue), again because Q_1 is very small i.e. in this case, the observed distortion is almost entirely caused by the on-board auxiliaries, with Q_1 that is several times smaller.

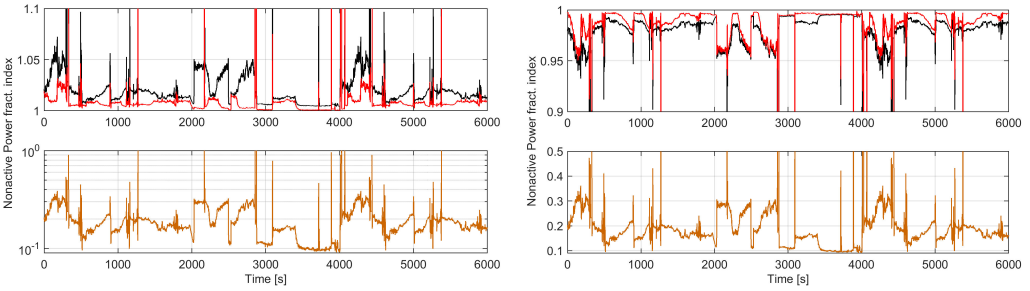

Fig. 6. Nonactive HPIs over a long run normalized to Q_1 (left, u_F (black), u_X (red), u_D (light brown)) and to Q_F (right, v_1 (black), v_X (red), v_D (light brown)) (Italy).

The Italian high-speed network has less traffic and a higher amount of installed power/train/km which results in less distortion and distortion terms vary much less as a function of the fundamental reactive power Q_1 (and total apparent power as well). In Fig. 5 the Q_X curve (red) is closer to Q_1 during intervals of significant absorption (when influence of auxiliaries is smaller and the power factor is optimized in nearly nominal conditions) and to Q_F when power absorption is lower. In any case, the numeric values of Q_1 and Q_F are quite close to each other (confirming RPII – rule 2), as shown in Table 1, so that identifying a suitable threshold requires some care i.e. with a consistent positioning of Q_X between the two areas at 65% and 22% on average, the suitable threshold is half-way around 40-45%.

Table 1. Positioning of Q_X within the Q_1-Q_F spread in % (ref. Fig. 5).

Quantity	t **= 1030 s**	t **= 1040 s**	t **= 1072 s**	t **= 1100 s**	t **= 1140 s**
Q_1 [MVA]	0.3820 (0%)	0.4563 (0%)	0.6445 (0%)	0.7016 (0%)	0.3639 (0%)
Q_X [MVA]	0.3855 (67.3%)	0.4604 (63.1%)	0.6476 (26.7%)	0.7045 (19.5%)	0.3664 (65.8%)
Q_F [MVA]	0.3872 (100%)	0.4628 (100%)	0.6561 (100%)	0.7165 (100%)	0.3677 (100%)

The application of RPII rules indicates that time intervals with large power absorption (such as 1072 s and 1100 s in Table 1) are recognized as “network distortion”, being Q_X much closer to Q_1 than to Q_F). Conversely, the other intervals with Q_X positioned closer to Q_F are tagged as “non-linear load”. The classification is correct in that at large power absorption the compliance to power factor limitation make the rolling stock a limited source of distortion which, instead, becomes more evident in relative terms when the power absorption is small. This is confirmed also for the Swiss 16.7 Hz system through inspection of the curves in Fig. 3.

The use of D as indicator is more ambiguous from Fig. 3 it is evident that when the power absorption is larger, D slightly increases as compared to the other scenarios, suggesting thus an opposite behaviour. In reality, what is relevant is the intensity of D compared to Q_F and Q_X, which, in turn, calls for the use of the normalized HPIs as indicators.

The normalized HPIs for nonactive power terms shown in Figs. 4 and 6 indicate that for distinguishing intervals with large distortion, the normalization by Q_F is preferable, as the v_1 curve (Q_1/Q_F, black) drops substantially below the upper bound 1 and the v_X curve (red). In Fig. 6(right) there can be seen a substantial similarity between the profiles of v_1 and v_X, that confirms that the 50 Hz system has lower distortion and almost no intervals where distortion at no traction load is particularly evident. As confirmation, see Fig. 6 (left) where normalization

is done with respect to Q_1, reports some intervals where u_F (black) detaches from u_X (red) and reaches values of 1.05, so 5% of nonactive distortion power, where level 1 is represented by Q_1. Conversely, for the 16.7 Hz system Fig. 4 (left) shows significant changes of more than an order of magnitude with respect to Q_1. Now, since the normalization is done with respect to Q_1, in time intervals where Q_1 drops to very small values the distortion levels are unavoidably amplified. This, however, does not happen in the 50 Hz system, for which, one can assume that the base consumption is much larger, preventing too small Q_1 values. As expected, the profile of v_D (normalized by Q_F) is complementary to v_1, as large distortion in percentage is observed when the fundamental reactive power (and thus overall power absorption) is small i.e. this is more evident for the 16.7 Hz system (see Fig. 4 (right)) than for the 50 Hz system (in Fig. 6 (right)).

5. Conclusions

This work has considered single-point HPIs based both on active and nonactive power terms and has evaluated them with measured voltage and current data taken at two European AC railways, in Switzerland and Italy. The purpose is to verify the applicability and effectiveness of such HPIs, in order to distinguish between harmonic components originating inside the rolling stock under test or caused by network distortion and possibly by other trains nearby.

The RPII-X index, based on the Q_X power term, as expected moves inside the channel defined by Q_1 and Q_F, that for low-distortion networks can be quite narrow i.e. observed variations are between 20 and 70% of the channel width (see Table 1). It is shown that situations of "network distortion" can be distinguished from those of "non-linear load", the latter indicating the rolling stock as a significant source of distortion, evaluated in relative terms; it is observed that with respect to the nominal power such distortion remains small. This index alone, however, is not able to separate distortion components by their origin.

The DPI index using distortion power D has a reasonable behaviour similar to the distortion part of Q_X, but it is not effective as long as its boundaries are not identified and justified (see Fig. 3(right) in particular). Its dynamic range is limited, although larger D values indicate situations of significant distortion, but necessitate a comparison with Q_X and Q_F for interpretation. The quantity D does not give indications of the source.

The API index, based on the harmonic active power, gives a thorough representation of harmonic components including the sign of the active power and lends itself to display graphically the bi-directional power flow between the rolling stock and the network, effectively covering also regenerative braking operation. The behaviour is consistent in both 16.7 and 50 Hz systems, although their distribution of harmonics is different (see Fig. 1 and Fig. 2). The sign of this index indicates the origin of the specific harmonic power (internal or external to the rolling stock); the relevance of a power term is indicated by its intensity, usually higher for harmonics of internal origin. The API index can be used to identify the characteristic harmonics of a specific train better than diagrams based on voltage and current vectors [14].

References

[1] Bongiorno, J., Boschetti, G., & Mariscotti, A. (2016). Low-Frequency Coupling: Phenomena in Electric Transportation Systems, *IEEE Electrification Magazine, 4*(3), 15–22. https://doi.org/10.1109/MELE.2016.2584959

[2] Mariscotti, A. (2019). Behaviour of Spectral Active Power Terms for the Swiss 15 kV 16.7 Hz Railway System. *Proceedings of 10th 2019 IEEE 10th International Workshop on Applied Measurements for Power Systems (AMPS)*, Aachen, Germany. https://doi.org/10.1109/AMPS.2019.8897777

[3] Mariscotti, A. (2019). Characterization of Active Power Flow at Harmonics for AC and DC Railway Vehicles. *Proceedings of IEEE Vehicle Power and Propulsion Conference (VPPC)*, Vietnam. https://doi.org/10.1109/VPPC46532.2019.8952310

[4] Mariscotti, A. (2020). Impact of Harmonic Power Terms on the Energy Measurement in AC Railways. *IEEE Transactions on Instrumentation and Measurement, 69*(9), 6731–6738. https://doi.org/10.1109/TIM.2020.2992167

[5] Mariscotti, A. (2020). Uncertainty of the Energy Measurement Function deriving from Distortion Power Terms for a 16.7 Hz Railway. *Acta Imeko, 9*(2), 25–31. https://doi.org/10.21014/acta_imeko.v9i2.764

[6] Hinrichs, G., & Hegarty, J. (2016). Introduction of energy metering, settlement and billing at SBB, European Railway Review, 22(1), 39–41. https://www.globalrailwayreview.com/article/26308/introduction-of-energy-metering-settlement-and-billing-at-sbb/

[7] European Committee for Standards – Electrical. (2017). *Railway applications – Energy measurement on board trains* (EN 50463-2).

[8] European Committee for Standards – Electrical. (2012). *Railway Applications – Power supply and rolling stock – Technical criteria for the coordination between power supply (substation) and rolling stock to achieve interoperability* (EN 50388).

[9] Mariscotti, A. (2011). Direct Measurement of Power Quality over Railway Networks with Results of a 16.7 Hz Network. *IEEE Transactions on Instrumentation and Measurement, 60*(5), 1604–1612. https://doi.org/10.1109/TIM.2010.2089170

[10] Mariscotti, A. (2012). Results on the Power Quality of French and Italian 2x25 kV 50 Hz railways. *Proceedings of International Instrumentation & Measurement Technology Conference (I2MTC)*, Austria. https://doi.org/10.1109/I2MTC.2012.6229341

[11] European Committee for Standards – Electrical. (2017). *Railway Applications – Fixed installations and rolling stock – Technical criteria for the coordination between traction power supply and rolling stock to achieve interoperability – Part 1* (prEN 50388-1).

[12] Costa, F. R., Santos, I. N., Silva, S. F. P., & De Oliveira, I. C. (2009). A case study of sharing the harmonic voltage distortion responsibility between the utility and the consumer. *Proceedings of International Conference on Renewable Energies and Power Quality*, Spain. https://doi.org/10.24084/repqj07.327

[13] Davis, E. J., Emanuel, A. E., & Pileggi, D. J. (2000). Evaluation of Single-Point Measurements Method for Harmonic Pollution Cost Allocation. *IEEE Transactions on Power Delivery, 15*(1), 14–18. https://doi.org/10.1109/61.847222

[14] Mariscotti, A. (2021). Experimental characterization of active and nonactive harmonic power flow of AC rolling stock and interaction with the supply network. *IET Electrical Systems in Transportation*.

[15] da Silva, R. P. B., Quadros, R., Shaker, H. R., & da Silva, L. C. P. (2019). Analysis of the Electrical Quantities Measured by Revenue Meters under Different Voltage Distortions and the Influences on the Electrical Energy Billing, *Energies, 12*, 4757. https://doi.org/10.3390/en12244757

[16] Olencki, A., & Mroz, P. (2014). Testing of energy meters under three-phase determined and random nonsinusoidal conditions. *Metrology and Measurement Systems, 21*(2), 217–232. https://doi.org/10.2478/mms-2014-0019

[17] Oliveira, L. T. S., de Oliveira, R. F. B., Macedo, J. R., & Leal, G. (2018). Performance analysis of active energy meters in non-sinusoidal conditions, *Proceedings of Simposio Brasileiro de Sistemas Eletricos (SBSE)*, Brazil. https://doi.org/10.1109/SBSE.2018.8395631

[18] Cataliotti, A., Cosentino, V., Lipari, A., & Nuccio, S. (2009). Metrological Characterization and Operating Principle Identification of Static Meters for Reactive Energy: an Experimental Approach under Nonsinusoidal Test Conditions. *IEEE Transactions on Instrumentation and Measurement, 58*(5), 1427–1435. https://doi.org/10.1109/TIM.2008.2009134

[19] Kosobudzki, G., Nawrocki, Z., & Nowak, J. (2005). Measure of Electric Reactive Power. *Metrology and Measurement Systems, 12*(5), 131–150.

[20] Czarnecki, L. S. (1993). Physical Reasons of Currents RMS Value Increase in Power Systems with Nonsinusoidal Voltage. *IEEE Transactions on Power Delivery, 8*(1), 437–447. https://doi.org/10.1109/61.180366

[21] Xu, W., Liu, X., & Liu, Y. (2003). An Investigation on the Validity of Power-Direction Method for Harmonic Source Determination. *IEEE Transactions on Power Delivery, 18*(1), 214–219. https://doi.org/10.1109/TPWRD.2002.803842

[22] Barbaro, V., Cataliotti A., Cosentino V., & Nuccio S. (2007). A Novel Approach Based on Nonactive Power for the Identification of Disturbing Loads in Power Systems. *IEEE Transactions on Power Delivery, 22*(3), 1782–1789. https://doi.org/10.1109/TPWRD.2007.899624

[23] Cataliotti A., & Cosentino V. (2009). Disturbing loads identification in power systems: a single-point time-domain method based on the IEEE 1459-2000. *IEEE Transactions on Instrumentation and Measurement, 58*(5), 1436–1445. https://doi.org/10.1109/TIM.2009.2015180

[24] Cataliotti, A., & Cosentino, V. (2009). A single-point approach based on IEEE 1459-2000 for the identification of prevailing harmonic sources detection in distorted three phase power systems. *Metrology and Measurement Systems, 16*(2), 209–218.

[25] Cataliotti, A., & Cosentino, V. (2010). A New Measurement Method for the Detection of Harmonic Sources in Power Systems based on the Approach of the IEEE Std. 1459–2000. *IEEE Transactions on Power Delivery, 25*(1), 332–340. https://doi.org/10.1109/TPWRD.2009.2034480

[26] Balci, M.E., & Hocaoglu, M.H. (2013). A Current Decomposition-Based Method for Computationally Efficient Implementation of Power Resolution Meters in Nonsinusoidal Single-Phase Systems. *Metrology and Measurement Systems, 20*(2), 263–274. https://doi.org/10.2478/mms-2013-0023

[27] Stevanović, D., & Petković, P. (2014). A single-point method based on distortion power for the detection of harmonic sources in a power system. *Metrology and Measurement Systems, 21*(1), 3–14. https://doi.org/10.2478/mms-2014-0001

[28] IEEE (2010). *IEEE Standard Definitions for the Measurement of Electric Power Quantities under Sinusoidal, Nonsinusoidal, Balanced, or Unbalanced Conditions* (IEEE Std 1459). https://doi.org/10.1109/IEEESTD.2010.5439063

[29] Hemmer, B., Mariscotti, A., & Wuergler, D. (2004). Recommendations for the calculation of the total disturbing return current from electric traction vehicles. *IEEE Transactions on Power Delivery, 19*(2), 1190–1197. https://doi.org/10.1109/TPWRD.2003.822962

[30] Richter, M., Komarnicki, P., & Hauer, I. (2018). Improving state estimation in smart distribution grid using synchrophasor technology: a comparison study. *Archives of Electrical Engineering, 67*(3), 469–483. https://doi.org/10.24425/123657

[31] Zajkowski, K., & Scaticailov, S. (2016). Determination of the environmental impact of reactive power compensation in the power grid. *Nonconventional Technologies Review, 20*(2), 54–61.

[32] Agamloh, E. B. (2017). Power and Efficiency Measurement of Motor-Variable-Frequency Drive Systems. *IEEE Transactions on Industry Applications, 53*(1), 766–773. https://doi.org/10.1109/TIA.2016.2602807

[33] Mazzanti, G., Passarelli. G., Russo, A., & Verde, P. (2006). The effects of voltage waveform factors on cable life estimation using measured distorted voltages. *Proceedings of IEEE Power Engineering Society General Meeting*, Canada. https://doi.org/10.1109/PES.2006.1709033

[34] Emanuel, A. E., & Wang, X. (1985). Estimation of Loss of Life of Power Transformers Supplying Nonlinear Loads. *IEEE Transactions on Power Apparatus and Systems, 104*(3), 628–636. https://doi.org/10.1109/TPAS.1985.318998

[35] Hu, H., Shao, Y., Tang, L., Ma, J., He Z., & Gao, S. (2018). Overview of Harmonic and Resonance in Railway Electrification Systems. *IEEE Transactions on Industry Applications, 54*(5), 5227–5245. https://doi.org/10.1109/TIA.2018.2813967

[36] Sharon, D. (1973). Reactive power definitions and power factor improvement in nonlinear systems. *Proceedings of the Institution of Electrical Engineers*, 120(6), 704–706. https://doi.org/10.1049/piee.1973.0155

[37] Farhoodnea, M., Mohamed, A., & Shareef, H. (2011). A Single Point Measurement Method for Evaluating Harmonic Contributions of Utility and Customer in Power Distribution Systems. *Journal of Applied Sciences, 11*(2), 257–265. https://doi.org/10.3923/jas.2011.257.265

[38] Ferrari, P., Mariscotti, A., & Pozzobon, P. (2000). Reference curves of the pantograph impedance in DC railway systems. IEEE International Symposium on Circuits and Systems (ISCAS), Switzerland. https://doi.org/10.1109/ISCAS.2000.857155

[39] Bongiorno, J, Mariscotti, A. (2015). Evaluation of performances of indexes used for validation of simulation models based on real cases. *International Journal of Mathematical Models and Methods in Applied Sciences, 9*, 29–43.

[40] Robert, A., Deflandre, T., Gunther, E., Bergeron, R., Emanuel, A., Ferrante, A., Finlay, G. S., Gretsch, R., Guarini, A., Gutierrez Iglesias, J. L., Hartmann, D., Lahtinen, M., Marshall, R., Oonishi, K., Pincella, C., Poulsen, S., Ribeiro, P., Samotyj, M., Sand, K., & Zhelesko, Y. S. (1997). Guide for Assessing the Network Harmonic Impedance. *14th International Conference and Exhibition on Electricity Distribution. Part 1. Contributions*, United Kingdom. https://doi.org/10.1049/cp:19970473

[41] Mariscotti, A., Giordano, D., Delle Femine, A., & Signorino, D. (2020). Filter Transients onboard DC Rolling Stock and Exploitation for the Estimate of the Line Impedance. *Proceedings of International Instrumentation & Measurement Technology Conference (I2MTC)*, Croatia. https://doi.org/10.1109/I2MTC43012.2020.9128903

[42] Crotti, G., Delle Femine, A., Gallo, D., Giordano, D., Landi, C., Luiso, M., Mariscotti, A. & Roccato, P. E. (2019). Pantograph-to-OHL Arc: Conducted Effects in DC Railway Supply System. *IEEE Transactions on Instrumentation and Measurement, 68*(10), 3861–3870. https://doi.org/10.1109/TIM.2019.2902805

[43] Mariscotti, A., & Giordano, D. (2020). Experimental Characterization of Pantograph Arcs and Transient Conducted Phenomena in DC Railways. *Acta Imeko, 9*(2), 10–17. https://doi.org/10.21014/acta_imeko.v9i2.761

[44] Wu, G., Wu, J., Wei, W., Zhou, Y., Yang, Z. & Gao, G. (2018). Characteristics of the Sliding Electric Contact of Pantograph/Contact Wire Systems in Electric Railways. *Energies, 11*(1), 17. https://doi.org/10.3390/en11010017

[45] Mariscotti, A. (2020). Data sets of measured pantograph voltage and current of European AC railways. *Data in Brief, 30*, 105477. https://doi.org/10.1016/j.dib.2020.105477

[46] International Electrotechnical Commission. (2008). *Electromagnetic compatibility (EMC) – Part 4-7: Testing and measurement techniques – General guide on harmonics and interharmonics measurements and instrumentation, for power supply systems and equipment connected thereto* (IEC 61000-4-7).

[47] Boschetti, G., & Mariscotti, A. (2012). Integrated Electromechanical Simulation of Traction Systems: Relevant Factors for the Analysis and Estimation of Energy Efficiency. *Proceedings of Electrical Systems for Aircraft, Railway and Ship Propulsion (ESARS)*, Italy. https://doi.org/10.1109/ESARS.2012.6387412

[48] Bigharaz, M. H., Hosseinian, S. H., Afshar A., Suratgar, A. A., & Dehcheshmeh, M. A. (2019). A comprehensive simulator of AC autotransformer electrified traction system. *International Journal of Power and Energy Conversion, 10*(2), 129–147. https://doi.org/10.1504/IJPEC.2019.098619

Andrea Mariscotti received the degree in Electronics Eng. in 1991 (cum laude) and the Ph.D. in Electrical Eng. in 1997 from the University of Genova. As a Tenure researcher and Assistant professor since 2005 he has worked in national and international research programs in the field of: EMC applied to industrial, military and transportation systems, including system assurance and functional safety aspects; power quality and power system modeling and analysis; electrical measurements, including the design and construction of measurement setups and instrumentation; earthing, stray current and lightning protection design and test for electrified transports.